UCLA
COMPUTATIONAL AND APPLIED MATHEMATICS

Level Set Method for Optimization Problems Involving Geometry and Constraints I. Frequencies of a Two-Density Inhomogeneous Drum

Stanley J. Osher
Fadil Santosa

August 2000

CAM Report 00-31

Department of Mathematics
University of California, Los Angeles
Los Angeles, CA. 90095-1555

http://www.math.ucla.edu/applied/cam/index.html

Level Set Methods for Optimization Problems Involving Geometry and Constraints I. Frequencies of a Two-Density Inhomogeneous Drum*

Stanley J. Osher† Fadil Santosa‡

Abstract

Many problems in engineering design involve optimizing the geometry to maximize a certain design objective. Geometrical constraints are often imposed. In this paper, we use the level set method devised in [11], the variational level set calculus presented in [20], and the projected gradient method, as in [15], to construct a simple numerical approach for problems of this type. We apply this technique to a model problem involving a vibrating system whose resonant frequency or whose spectral gap is to be optimized subject to constraints on geometry. Our numerical results are quite promising. We expect to use this approach to deal with a wide class of optimal design problems in the future.

1 Introduction and problem statement

This work is motivated by the need to develop methods for solving optimization problems in engineering design. Many of these problems involve optimizing the geometry to maximize a certain design objective. Constraints, often involving geometry, are imposed. Therefore, the problems can be viewed as constrained optimization.

An example of such a problem arises in structural engineering. Here, a structure is assigned to support a given load. The objective is to make the structure as light as possible while satisfying a compliance constraint, which could be stated as displacing a fixed amount for a given load [3, 14, 4]. Such

*The research of SJO is supported in part by DARPA/NSF VIP Grant NSF DMS9615854, NSF DMS0074735 and ARO DAAG 55-98-1-0323. The research of FS is supported in part by an AFOSR/MURI Grant to the University of Delaware.

†Department of Mathematics, University of California, Los Angeles, 520 Portola Plaza, Los Angeles, CA 90095-1555, USA.

‡School of Mathematics, University of Minnesota, 206 Church St SE, Minneapolis, MN 55455, USA.

problems have been studied extensively and it has been shown that the optimal solution is a composite in the sense that it has microstructures [2].

Other applications of the techniques developed here include design of photonic bandgap devices [8].

Here we consider a model problem of structural vibration control [3, 14]. We are given a vibrating system whose resonant frequencies may lie in some undesirable window. We are allowed to change the geometry of the structure, or add mass to it, in order to push the resonant frequencies away from the prespecified window. The constraint may be geometrical – the structure must have certain topology, or it may be for other consideration – the total mass we add to the structure must be fixed.

Another problem we consider is one where the structure has the desired resonant frequency gap, and our goal is to find a 'simpler' design that still possess the desired gap.

To demonstrate the main ideas of our approach, we study the following eigenvalue problem. Consider a drum head with a fixed shape $\Omega \in \mathbb{R}^2$ and variable density $\rho(x)$. The resonant frequencies of the drum is found by solving the eigenvalue problem

$$-\triangle u = \lambda \rho(x) u, \quad x \in \Omega, \tag{1a}$$

$$u = 0, \quad x \in \partial\Omega. \tag{1b}$$

Let $S \subset\subset \Omega$ be a domain inside Ω. We do not assume any topology on S. We assume that the density $\rho(x)$ takes on two values

$$\rho(x) = \begin{cases} \rho_1 & \text{for} \quad x \notin S \\ \rho_2 & \text{for} \quad x \in S \end{cases} . \tag{2}$$

We will deal only with the first two eigenvalues λ_1 and λ_2. For simplicity, we assume that they are distinct, and that λ_2 is separated from λ_3 for any S. We shall relax this assumption in future work.

The optimization problems we want to consider are as follows.

Problem 1: Solve the optimization

$$\max_S \lambda_1 \quad \text{or} \quad \min_S \lambda_1 \quad \text{or} \quad \max_S (\lambda_2 - \lambda_1),$$

subject to the constraint

$$\|S\| = K,$$

where K is a prescribed number. This problem is a cartoon of the structural vibration control that we described earlier.

Problem 2: Solve the optimization

$$\min_S \|S\| \quad \text{subject to} \quad \lambda_2 - \lambda_1 = M.$$

Here M is a fixed number. This represents the 'simplification of a design' problem alluded to above.

The challenge in solving these problems come in the fact that we do not know the topology of S. To overcome this, we use the level set approach proposed by Osher and Sethian [11]. The method provides an efficient way of describing time evolving curves and surfaces which may undergo topological change. Another challenge is the presence of one or more constraints in the optimization. We tackle this difficulty by modifying the projected gradient method devised for deblurring and denoising of images by Rudin, Osher and Fatemi [15]. The modification comes in the fact that we use Newton's method to project back into the constraint manifold after we 'stray' too far from it.

Therefore, viewed at a high level, this work presents a method for dealing with optimal design problems involving geometry and constraints. We note that Sethian and Wiegmann [17] studied the problem of structural optimization using level sets. What sets the present work apart are the use of functional gradients to calculate the velocity of the level set, and the precise way we deal with the hard constraints.

Theoretical issues concerning Problem 1 have been investigated by Cox and McLaughlin [9]. They addressed the existence of extrema, and provided a characterization of the extremal solution using the nodal domains of the eigenfunctions. A numerical algorithm for minimizing the first eigenvalue based on this theoretical work has been implemented in [6]. Cox [7] also studied the gradients of the eigenvalues with respect to a distributed density, and in particular, consider the case where an eigenvalue is repeated. For the case of two-density domains, the functional analysis of the gradients of the eigenvalues and constraints still needs to be done. We note the work of Sokolowski and Zolesio [18] which addresses differentiability of certain functionals with respect to geometry. The results of their work may well be applicable to the present problem. However, we defer investigation of the more theoretical aspects of this problem. Instead, we will focus on developing effective numerical schemes for the problems stated.

2 Level set formulation and the projected gradient approach

A key idea that makes the optimization tractable is to represent the unknown set S as the level set of a function $\phi(x)$ where

$$S := \{x : \phi(x) > 0\}. \tag{3}$$

Then $\rho(x)$ in (2) is given by

$$\rho(x) = \begin{cases} \rho_1 & \text{for} \quad \{x : \phi(x) < 0\} \\ \rho_2 & \text{for} \quad \{x : \phi(x) > 0\} \end{cases} . \tag{4}$$

We will now work with function $\phi(x)$ instead of $\rho(x)$.

The generic optimization problem we need to solve is

$$\min F(\phi) \quad \text{subject to } G(\phi) = 0. \tag{5}$$

If we are solving Problem 1, then $F(\cdot)$ represents an objective associated with the eigenvalues of (1), and $G(\cdot)$ represents the constraint on the mass, which we rewrite as

$$G(\phi) = \int_{\{x:\phi>0\}} 1 \, dx - K.$$

For Problem 2, we take

$$F(\phi) = \int_{\{x:\phi>0\}} 1 \, dx,$$

and $G(\phi) = \lambda_2 - \lambda_1$. In summary, what we need to address is an optimization involving a nonquadratic functional and a single nonlinear constraint. We emphasize that several of the problems described in [14, 3] fall into this class.

We use the Lagrange Multiplier Method to solve the optimization problem (5). The Lagrangian, with multiplier ν is given by

$$L(\phi, \nu) = F(\phi) + \nu G(\phi). \tag{6}$$

The necessary condition for a minimizer is

$$D_\phi L(\phi, \nu) = D_\phi F(\phi) + \nu D_\phi G(\phi) = 0. \tag{7a}$$

This, together with the constraint

$$G(\phi) = 0, \tag{7b}$$

allows us, in principle, to find ϕ and ν. Next we address the issue of how to formally compute the gradients of F and G with respect to ϕ.

2.1 Gradient calculations

To facilitate the calculation of the gradient of F with respect to ϕ, we observe that F is a function of ρ, which is given implicitly in terms of ϕ through (4). We will use the chain rule

$$D_\phi F(\phi) = D_\rho F \, D_\phi \rho,$$

because the derivative of F with respect to ρ is straightforward.

As an example, let $F(\phi) = \lambda_1$. Then, the eigenpair (u_1, λ_1) solves

$$\begin{aligned} -\triangle u_1 &= \lambda_1 \rho(x) u_1, \quad x \in \Omega, \\ u_1 &= 0, \quad x \in \partial\Omega. \end{aligned}$$

A variation in the density by an amount $\delta\rho$ results in variations in u_1 and λ_1. We denote these by δu_1 and $\delta\lambda_1$. Applying the variation to the partial differential equation leads to

$$-\triangle \delta u_1 = \lambda_1 \rho(x) \delta u_1 + \delta\lambda \rho u_1 + \lambda_1 \delta\rho(x) u_1.$$

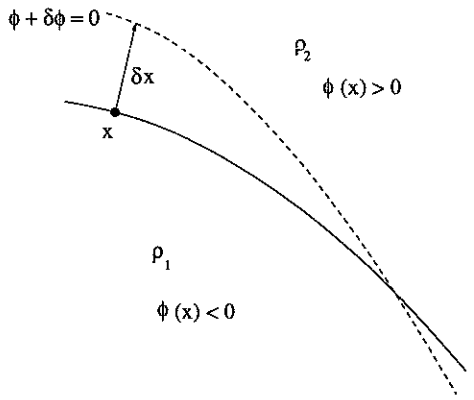

Figure 1: The geometry of the zero level set under variation in ϕ.

Rearranging, we have

$$-\Delta\delta u_1 - \lambda_1\rho(x)\delta u_1 = \delta\lambda_1\rho u_1 + \lambda_1\delta\rho(x)u_1.$$

For the equation above to yield a nontrivial δu_1, the right-hand side must be orthogonal to u_1. This implies that

$$D_\rho\lambda_1 \cdot \delta\rho = \delta\lambda_1 = -\frac{\lambda_1 \int_\Omega \delta\rho(x)u_1^2\, dx}{\int_\Omega \rho(x)u_1^2\, dx}. \tag{8}$$

For functionals F involving λ_1 and λ_2, we can proceed in a similar way.

The calculation for the gradient of ρ with respect to ϕ is more complicated. There are several ways to proceed. The approach presented by Zhao et al [20] is an effective way of dealing with such a calculation. Here, we follow the derivation outlined in [16]. We begin by studying the geometry of the zero level set, $\partial S = \{x : \phi(x) = 0\}$ under a variation in ϕ. Consider the situation depicted in Figure 1. The solid curve is the zero level set before ϕ is varied; the dashed curve is the zero level set of $\phi + \delta\phi$. Suppose the set S become S' under the variation in ϕ. A point x on the zero level set has been displaced by δx.

The variation $\delta\rho$ is integrated against a test function $f(x)$

$$< \delta\rho, f >:= \int_\Omega \delta\rho(x)\, f(x)\, dx = \int_{\text{symdiff}(S,S')} \delta\rho(x)\, f(x)\, dx,$$

where $\text{symdiff}(S, S') = (S \cup S') \setminus (S \cap S')$ is the symmetric difference of the sets S and S'. Because the difference in S and S' is infinitesimal, we can reduce the area integral to a line integral. Let $n(x) = \nabla\phi/|\nabla\phi|$ denote the inward normal to S. We use the fact that $\delta\rho(x)$ is either plus or minus $(\rho_2 - \rho_1)$; plus when $\delta x \cdot n(x)$ is negative, and minus otherwise. Therefore, the integral becomes

$$< \delta\rho, f >= -\int_{\partial S} (\rho_2 - \rho_1)\, \delta x \cdot n(x)\, f(x)\, ds(x),$$

where $ds(x)$ is the incremental arclength.

We can now identify $\delta\rho$ from the last expression as

$$\delta\rho = -\left(\rho_2 - \rho_1\right) \frac{\nabla\phi(x)}{|\nabla\phi(x)|} \cdot \delta x \Big|_{x\in\partial S}.$$

To remove δx from the expression, we take the variation of the equation $\phi(x) = 0$,

$$\delta\phi + \nabla\phi \cdot \delta x = 0. \tag{9}$$

Therefore, we arrive at

$$\delta\rho = D_\phi\, \rho \cdot \delta\phi = \left(\rho_2 - \rho_1\right) \frac{\delta\phi}{|\nabla\phi|}\Big|_{x\in\partial S}. \tag{10}$$

We interpret the result as saying that when $\phi(x)$ is varied, the variation in $\rho(x)$ occurs only along the zero level set ∂S.

Putting the results in (8) and (10) together, we get

$$D_\phi\lambda_1 \cdot \delta\phi = \frac{\lambda_1(\rho_2 - \rho_1)}{\int_\Omega \rho u_1^2\, dx} \int_{\partial S} \frac{u_1^2}{|\nabla\phi|}\, \delta\phi\, ds(x). \tag{11}$$

The same procedure can be applied to obtain gradients of objective functional F which involve λ_1 and λ_2.

In Problem 1, $G(\phi) = \int_S dx - K$. To calculate the variation of $G(\phi)$, we need to come up with an expression for the variation of the area of S. We refer to Figure 1. We observe that the change in area at x is positive if $\delta x \cdot n(x) < 0$, and negative otherwise. The total change in area then is given by

$$-\int_{\partial S} \delta x \cdot n(x)\, ds(x).$$

Using (9) and $n(x) = \nabla\phi/|\nabla\phi|$, we get

$$D_\phi G(\phi) \cdot \delta\phi = \int_{\partial S} \frac{\delta\phi}{|\nabla\phi|}\, ds(x). \tag{12}$$

The gradient formulas will be needed in devising a computational algorithm for optimization, which we describe next.

2.2 Projected gradient algorithm

The surface $\phi(x)$ will be altered so that points on a level curve will move perpendicular to it. This means that the change is given by the expression

$$\delta\phi + v(x)|\nabla\phi| = 0.$$

The above is equivalent to a Hamilton-Jacobi equation if we view the change as occurring continuously in time. The function $v(x)$ represents the velocity of the level curves.

Choosing the velocity field $v(x)$ amounts to choosing a descent direction for the optimization. We choose the steepest descent direction. For the example where $F(\phi) = \lambda_1$, we find, from (11) and (12) that

$$\begin{aligned} D_\phi L \cdot \delta\phi &= D_\phi \lambda_1 \cdot \delta\phi + \nu D_\phi G(\phi) \cdot \delta\phi \\ &= \int_{\partial S} \left\{ \frac{\lambda_1(\rho_2 - \rho_1)}{\int_\Omega \rho u_1^2 \, dx} u_1^2 + \nu \right\} \frac{\delta\phi}{|\nabla\phi|} \, ds(x). \end{aligned} \tag{13}$$

Now we set

$$\delta\phi = -\left(\frac{\lambda_1(\rho_2 - \rho_1)}{\int_\Omega \rho u_1^2 \, dx} u_1^2 + \nu \right) |\nabla\phi|. \tag{14}$$

By substituting $\delta\phi$ given in (14) in equation (13), we can conclude that it is a descent direction. We can identify the velocity field $v(x)$ as

$$v(x) = \left(\frac{\lambda_1(\rho_2 - \rho_1)}{\int_\Omega \rho u_1^2 \, dx} u_1^2 + \nu \right). \tag{15}$$

It is important to note that we have 'naturally' extended the velocity from its value on the zero level set ∂S to the entire domain Ω exploiting the fact that $u_1(x)$ is defined in all of Ω. The only requirement for the velocity to correspond to a descent direction is for its value be as specified in (15) *only on* ∂S. Therefore, an alternate implementation is to define the velocity on the zero level set, and extend it to all of Ω by other means, such as the method outlined in [5, 20].

However, this descent direction may take the current estimate for $\phi(x)$ out of the feasible set. The value of the Lagrange multiplier will be set to keep $\phi(x) + \delta\phi(x)$ feasible. We use a projection approach which is based on the method described in Rudin, Osher and Fatemi [15] with a small modification. The projection is based on the linearization of the constraint equation $G(\phi) = 0$. We insist that any update must be tangent to this set; that is $\delta\phi$ must satisfy

$$D_\phi G(\phi) \cdot \delta\phi = 0. \tag{16}$$

For Problem 1, this amounts to a requirement on the velocity on the zero level set. To see this, we take the expression for the directional derivative of G in (12) and use $\delta\phi + v|\nabla\phi| = 0$. We get

$$\int_{\partial S} v(x) \, ds(x) = 0.$$

In implementation, we do not evaluate the contour integral. We use Stoke's identity to rewrite the contour integral as

$$\begin{aligned} \int_{\partial S} v(x) \, n(x) \cdot n(x) \, ds &= \int_{\partial S} v(x) \, \frac{\nabla\phi}{|\nabla\phi|} \cdot n(x) \, ds \\ &= \int_S \nabla \cdot \left(v(x) \frac{\nabla\phi}{|\nabla\phi|} \right) dx. \end{aligned}$$

Letting

$$v_0(x) = \frac{\lambda_1(\rho_2 - \rho_1)}{\int_\Omega \rho u_1^2 \, dx} u_1^2,$$

we obtain a formula for the Lagrange multiplier ν

$$\nu = -\int_S \nabla \cdot v_0(x) \frac{\nabla\phi}{|\nabla\phi|} \, dx \Big/ \int_S \nabla \cdot \frac{\nabla\phi}{|\nabla\phi|} \, dx.$$

The linearized constraint in terms of velocity has a natural interpretation. It states that for the total area of S to be conserved as required by the constraint, the total flux on the zero level set must be zero.

Remark Alternately, one can deal directly with contour integrals by first representing them with delta functions, and then replacing the delta functions with smoothed approximations. This approach is outlined in [20] and goes as follows. We write

$$\int_{\partial S} v(x) \, ds = \int_\Omega v(x)\delta(\phi(x))|\nabla\phi| \, dx.$$

This equality uses the fact that $\partial S = \{x : \phi(x) = 0\}$, and is formally justified. In computations, we approximate $\delta(x)$ by

$$\delta_h(x) = \begin{cases} 0 & \text{for} \quad |x| > h \\ \frac{1}{2h}\left[1 + \cos\left(\frac{\pi|x|}{h}\right)\right] & \text{for} \quad |x| \le h \end{cases}.$$

Thus, the line integral is approximated using an area integral.

The projection step, because we will be taking finite steps along the tangent to the feasible set, will eventually make the iterates infeasible. To put an iterate back onto the feasible set after it has 'drifted' too far away from the constraint set, we use Newton's method. With the unknown being ν, we write $\delta\phi(x;\nu)$ in (14) as a function of ν. Then we take steps

$$\nu \leftarrow \nu - \left(D_\nu G(\phi + \delta\phi(x,\nu))\right)^{-1} G(\phi + \delta\phi(x,\nu)).$$

Note that we only need to perform this step when an iterate has violated the constraint by a specified tolerance. Moreover, the ingredients needed to do the computation are already derived in the gradient calculations.

The approach outlined can be applied to Problem 2, as well as other types of constrained optimization problems involving more constraints. We summarize the method described above as an algorithm in Figure 2.

3 Numerical experiments

To test out the method for optimization as outlined in Section 2.2, we consider solving the problem on a rectangular domain $\Omega = [0,1] \times [0,1.5]$. We discretize Ω using a regular mesh. The update for the level surface $\phi(x)$ is given by

$$\delta\phi + v(x)|\nabla\phi| = 0,$$

initial guess for $\phi(x)$
do while not optimal
- compute $D_\phi F(\phi)$ and $D_\phi G(\phi)$
- solve for Lagrange multiplier ν in (16) (when needed, solve for ν via Newton's method)
- get descent direction $\delta\phi$
- update $\phi(x)$ to $\phi(x) + \alpha\delta\phi(x)$

Figure 2: Algorithm for solving $\min F(\phi)$ subject to $G(\phi) = 0$. Here $\alpha > 0$ is the step size.

where $v(x)$ is given by (15). We view this as a discrete-time Hamilton-Jacobi equation, with $\delta\phi$ representing the difference of ϕ at two time instances. The Hamiltonian is

$$H(x, \nabla\phi) = v(x)|\nabla\phi|.$$

The technology needed to solve such equations and accurately compute the correct (viscosity) solution, kinks and all, is quite advanced by now. Higher order ENO [12] and WENO [10] schemes are available. For problems involving interfaces, such as ours, we are only interested in the zero level set of $\phi(x)$. This means that we can evolve the interface efficiently by only solving the equation in the neighborhood of the zero level set. Methods which exploit this feature of the problem have been proposed in [1, 13]. Note that the function $\phi(x)$ is only in the computation to keep track of the interface defined by the zero level set. Because steep or flat slopes can develop in the evolution of $\phi(x)$ through the Hamilton-Jacobi equation, it is advantageous to reinitialize $\phi(x)$ using the signed distance to a zero level set in order regularize the function $\phi(x)$. This initialization, which does not affect the computation of the zero level set, increases the accuracy of the computation [19].

In the present work, this part of the calculation consumes only a small fraction of the computational effort. We do not implement the local method or the reinitialization. We simply adopt the simple monotone upwind scheme devised in [11]. The calculation of the eigenvalues and eigenfunctions associated with the objectives were done using Matlab routine `eigs`.

In all the experiments that follow, the mesh size is $\Delta x = \Delta y = 0.025$ (40×60 grid). The density is $\rho_1 = 1$ and $\rho_2 = 2$. The level set function is extended periodically over the region Ω. Because of the scaling in the eigenfunctions, we needed to adjust step size α to ensure stability. This number can be arrived at by considering the CFL condition. In our implementation for solving Problem 1, the Newton iteration is invoked each time we violate the constraint by more that 3 pixels. For Problem 2, the Newton iteration is used when we violate the gap constraint by more than 1%.

In the first example, we consider the problem of maximizing the first eigenvalue. We start with a density distribution shown in the upper left corner of Figure 4. In that figure, white corresponds to $\rho_2 = 2$. The value of λ_1 starts at

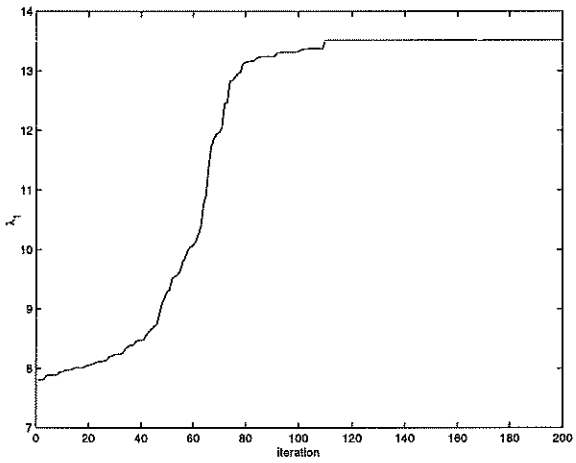

Figure 3: Maximization of λ_1; see Figure 4 for corresponding densities.

below 8. As we iterate, the eigenvalue increases until it reaches a stable value of around 13.5 after 200 iterations (see Figure 3). The density distribution as a function of iteration is displayed in Figure 4. Note the change in the topology of the region S as we iterate.

The second example demonstrates the process of minimizing the first eigenvalue. Starting with the same initial density distribution as in the previous example, the algorithm found the minimum eigenvalue, at a little below 7.4, after 400 iterations (see Figure 5). The density distribution as we progress towards the optimum is shown in Figure 6.

Next we consider the problem of maximizing the gap between λ_2 and λ_1. Starting with the initial density distribution in the upper left corner of Figure 8, we found the distribution that maximizes the gap in 400 iterations. The density distributions as we iterate are shown in Figure 8. It is instructive to examine the evolution of the gap as a function of iterations in Figure 7. We see that the second eigenvalue can be made larger at a modest cost of a small increase in the first eigenvalue.

The fourth example deals with minimizing the area of the S while maintaining a given gap. This is Problem 2 described in Section 1. The desired gap corresponds to $(\lambda_2 - \lambda_1)$ for the density distribution shown in the upper left corner of Figure 10. We show the reduction in the area of S as we iterate in Figure 9. Figure 10 displays the density distribution as a function of iterations. It is remarkable that everyone of the density distribution in Figure 10 has the same gap. To see this more clearly, in Figure 11 we show the eigenvalues λ_1 and λ_2 as we iterate. We note that they move in parallel as a function of iteration, leaving the gap constant.

The final example combines the optimization processes in Problem 1 and Problem 2. We use the density corresponding to the maximum gap in the third

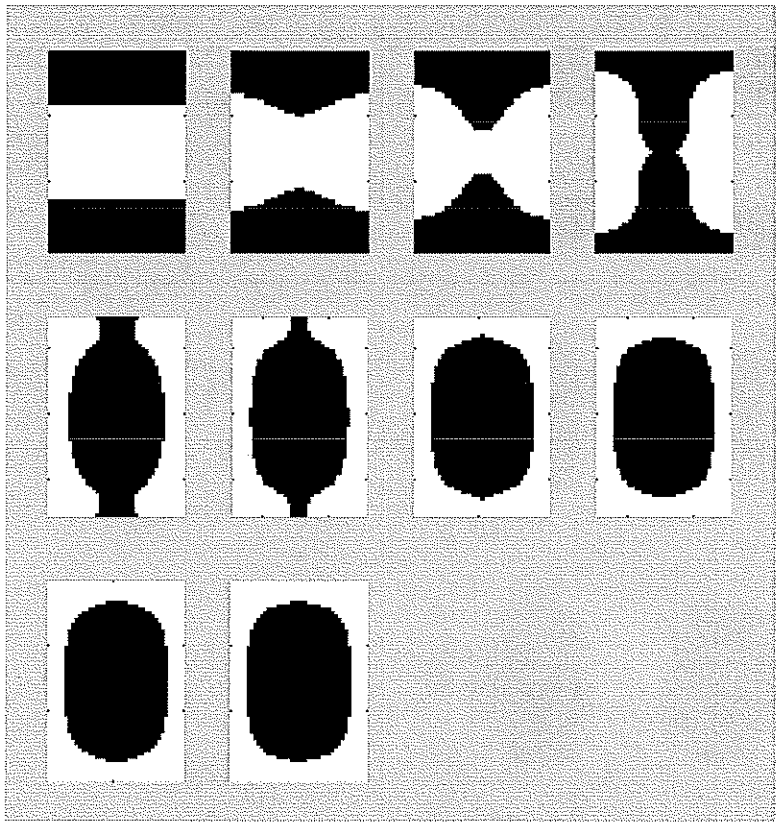

Figure 4: Maximization of λ_1: the densities as we iterate toward solution.

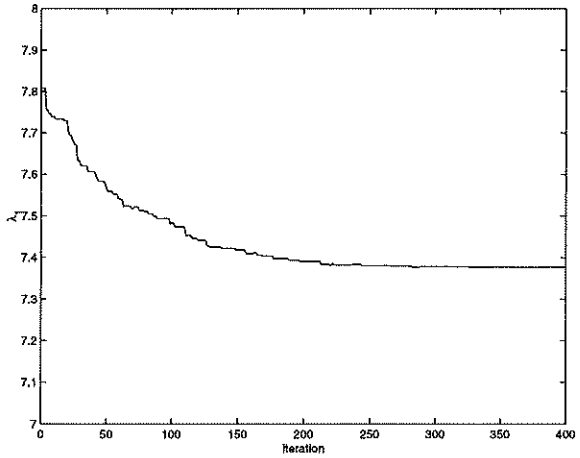

Figure 5: Minimization of λ_1; see Figure 6 for corresponding densities.

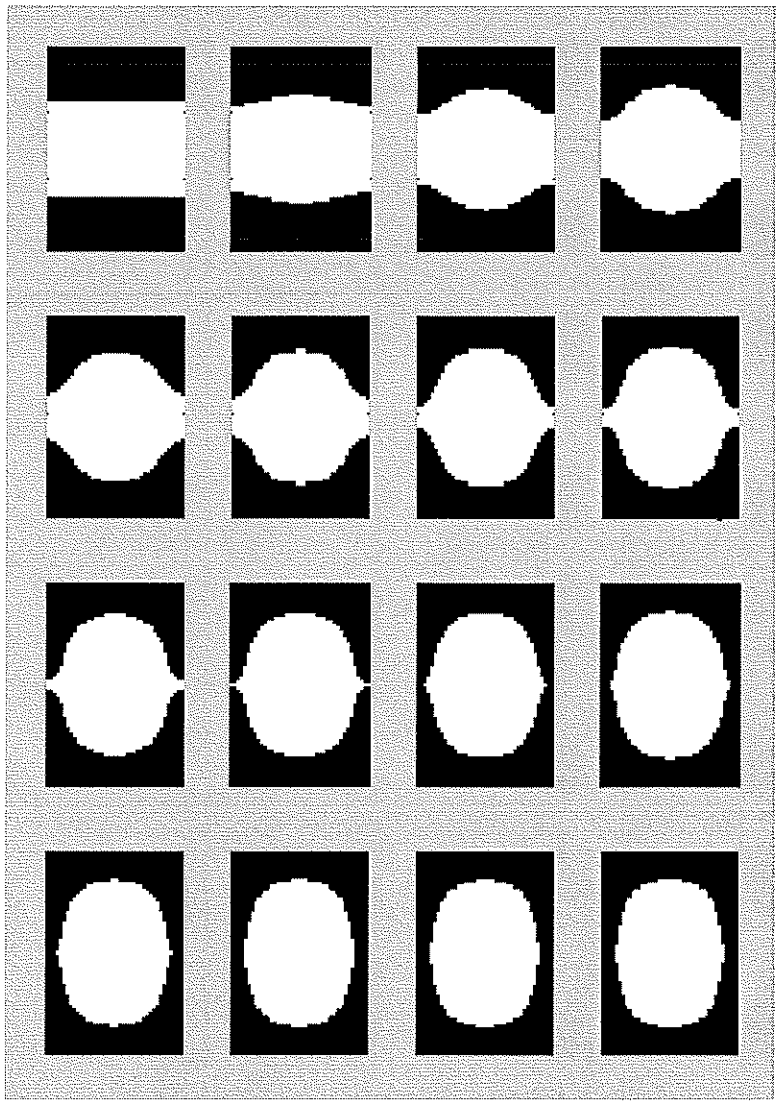

Figure 6: Minimization of λ_1: the densities as we iterate toward solution.

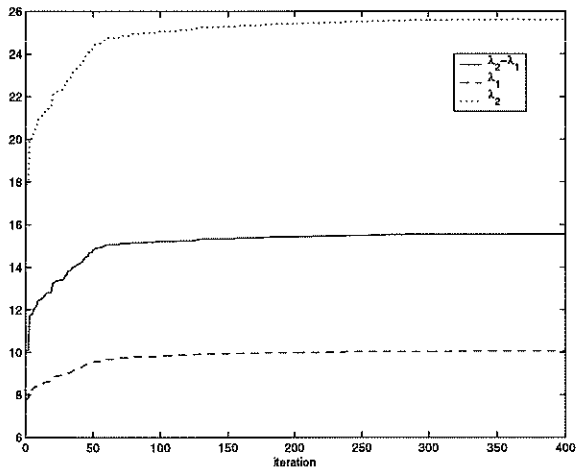

Figure 7: Maximization of $(\lambda_2 - \lambda_1)$; see Figure 8 for corresponding densities.

example, shown now in the upper left hand corner of Figure 13. Next, we take the gap as a constraint and reduce the area of S. The reduction in area, and the density distributions, as we iterate are shown in Figures 12 and 13. A density with small $\|S\|$ with the same gap is found. Figure 14 shows that the gap is maintained as we iterate.

4 Discussion

We have presented a method for solving optimal design problems involving geometry and constraints using the level set formulation. The optimization strategy is based on the projected gradient approach. We considered optimization problems involving eigenvalues of a two-density drum either in the objective or the constraint. The results we obtained are quite promising. We believe that the general approach presented here can be applied to a wide variety of optimal design problems involving geometry and constraints.

References

[1] D. Adalsteinsson and J. Sethian, A fast level set method for propagating interfaces, *J. Comput. Phys.*, **118**(1995), pp. 269–277.

[2] G. Allaire, The homogenization method for topology and shape optimization, in *Topology Optimization in Structural Mechanics*, Rozvany, ed., CISM, 1997.

[3] M. Bendsoe and C. Mota Soares, eds., *Topology Design of Structures*, Kluwer, Dordrecht 1993.

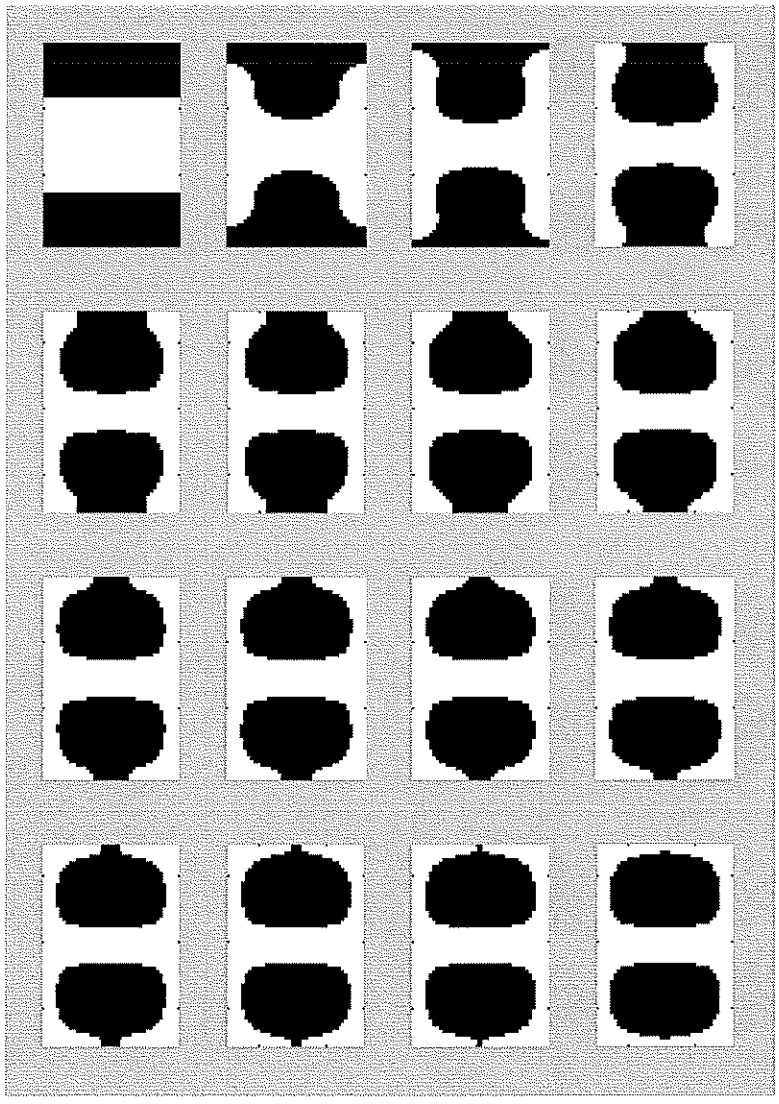

Figure 8: Maximization of $(\lambda_2 - \lambda_1)$: the densities as we iterate toward solution.

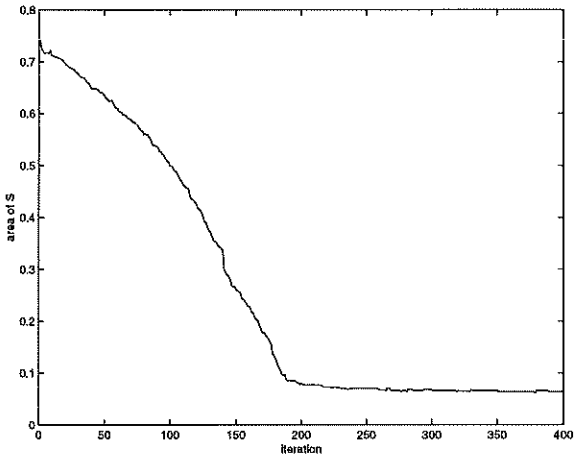

Figure 9: Minimization of $\|S\|$ subject to a fixed gap; see Figure 10 for the corresponding densities.

[4] M. Bendsoe, *Optimization of Structural Topology, Shape and Material*, Springer, Berlin, 1997.

[5] S. Chen, B. Merriman, S. Osher, and P. Smereka, A simple level set method for solving Stefan problems, *J. Comput. Phys.*, **135**(1997), pp. 8–29.

[6] S. Cox, The two phase drum with the deepest bass note, *Japan J. Industrial Applied Math.*, **8**(1991), pp. 345–355.

[7] S. Cox, Generalized gradient at a multiple eigenvalue, *J. Func. Anal.*, **130**(1995), pp. 30–40.

[8] S. Cox and D. Dobson, Band structure optimization of two-dimensional photonic crystals in H-polarization, *J. Comput. Phys.*, **158**(2000), pp. 214–224.

[9] S. Cox and J. McLaughlin, Extremal eigenvalue problems for composite membranes, I and II, *Applied Math. and Optimization*, **22**(1990), pp. 153–167, and pp. 169–187.

[10] G. Jiang and D. Peng, Weighted ENO schemes for Hamilton-Jacobi equations, *SIAM J. Sci. Comput.*, **21**(2000), pp. 2126–2143.

[11] S. Osher and J. Sethian, Front propagation with curvature-dependent speed: algorithms based on Hamilton-Jacobi formulations, *J. Comput. Phys.*, **79**(1988), pp. 12–49.

[12] S. Osher and C. Shu, High order essentially nonoscillatory schemes for Hamilton-Jacobi equations, *SIAM J. Numer. Anal.*, **28**(1991), pp. 907–922.

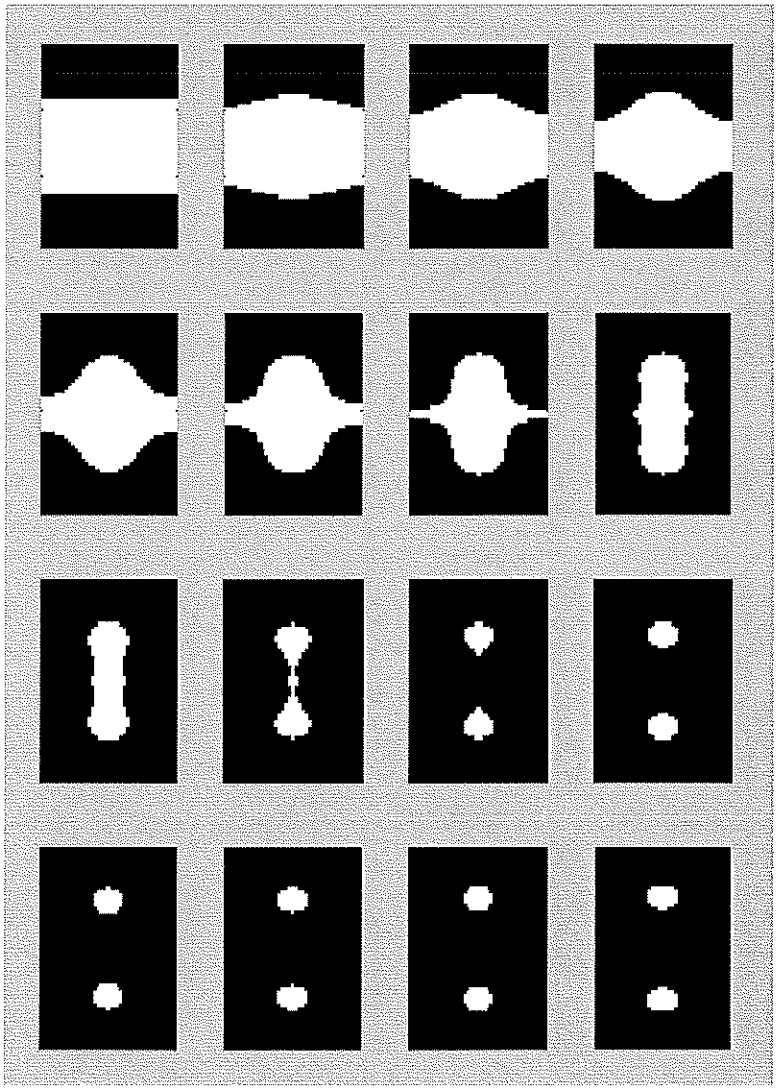

Figure 10: Minimization of $\|S\|$ subject to a fixed gap: the densities as we iterate towards solution. Note that all the densities shown have the same gap.

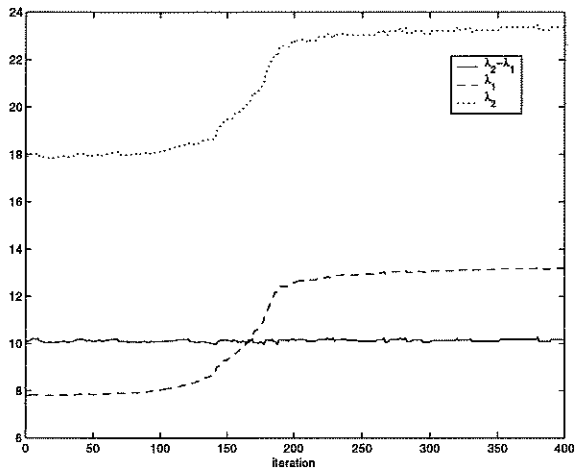

Figure 11: Minimization of $||S||$ subject to a fixed gap. Shown are the eigenvalues λ_1, λ_2 and the gap as we iterate. Note how the eigenvalues move in parallel.

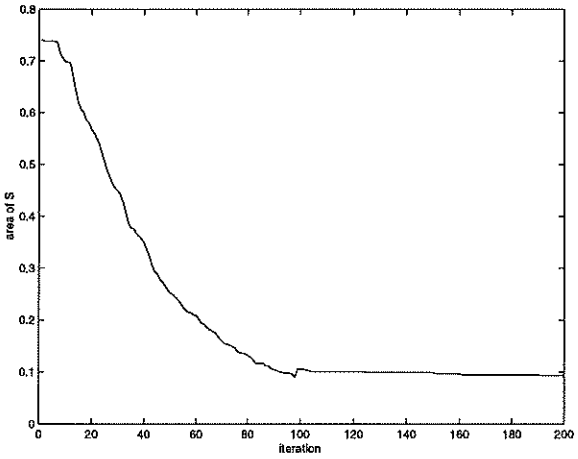

Figure 12: Minimization of $||S||$ subject to a fixed gap. The gap corresponds to the density that maximizes the gap for a fixed S in the third example.

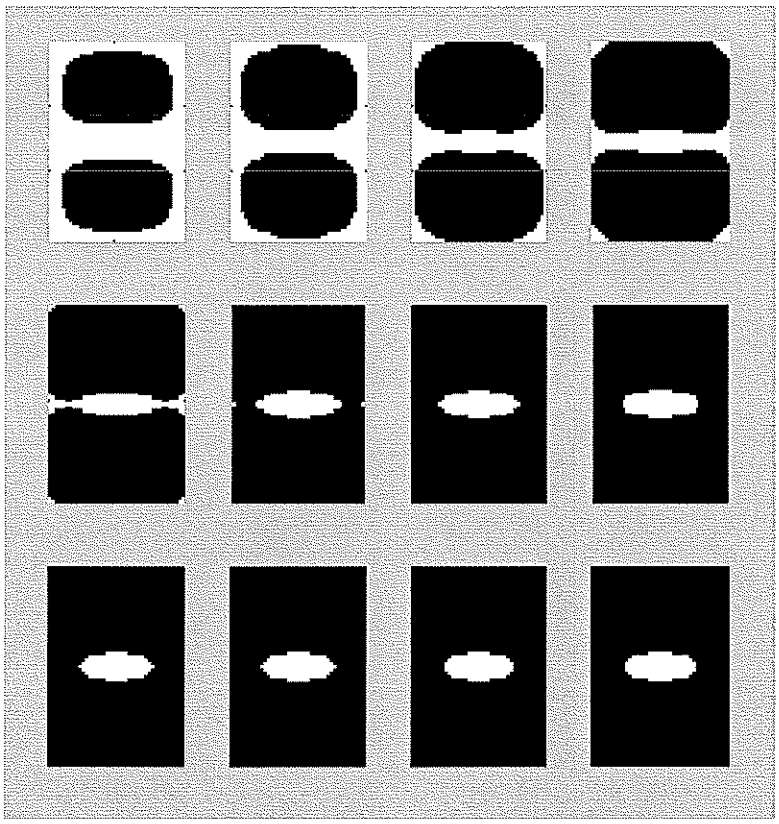

Figure 13: Minimization of $\|S\|$ subject to a fixed gap. Shown are the densities as a function of iterations. All the densities shown have the same gap.

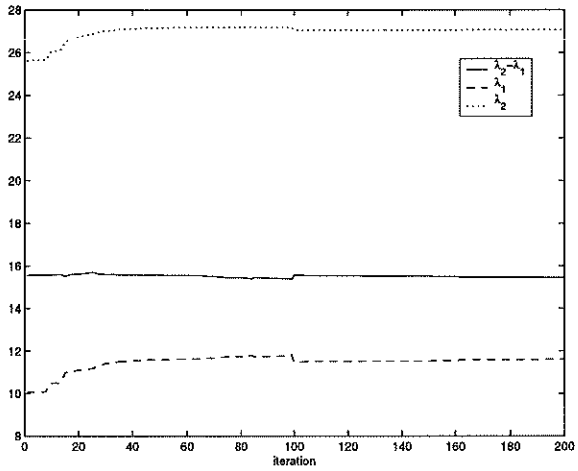

Figure 14: Minimization of $||S||$ subject to a fixed gap. This figure demonstrates that the constraint is observed during iterations.

[13] D. Peng, B. Merriman, S. Osher, H. Zhao, and M. Kang, A PDE-based fast local level set method, *J. Comput. Phys.*, **155**(1999), pp. 410–438.

[14] I. Rozvany, ed., *Topology Optimization in Structural Mechanics*, Springer, New York 1997.

[15] L. Rudin, S. Osher, and E. Fatemi, Nonlinear total variation based noise removal algorithms, *Physica D*, **60**(1992), pp. 259–268.

[16] F. Santosa, A level-set approach for inverse problems involving obstacles, *Control, Optimization, and Calculus of Variation*, **1**(1996), pp. 17–33.

[17] J. Sethian and A. Wiegmann, Structural boundary design via level set and immersed interface methods, Preprint 1999.

[18] J. Sokolowski and J.-P. Zolesio, *Introduction to Shape Optimization. Shape Sensitivity Analysis*, Springer, Heidelberg, 1992.

[19] M. Sussman, P. Smereka, and S. Osher, A level set approach for computing solutions to incompressible two-phase flow, *J. Comput. Phys.*, **114**(1994), pp. 146–159.

[20] H. Zhao, T. Chan, B. Merriman, and S. Osher, A variational level set approach to multiphase motion, *J. Comput. Phys.*, **127**(1996), pp. 179–195.